Violene/Cyanine Hybrids as Electrochromic Systems: A New Variation of the General Structure[‡]

Siegfried Hünig,*[a] Anja Langels,[a] Michael Schmittel,[b] Hermann Wenner,[a]
Igor F. Perepichka,[c] and Karl Peters[d]

Keywords: Violenes / Cyanines / Redox chemistry / Electrochromics / Heterocycles

The recently disclosed general structure of violene/cyanine hybrids is extended to a new variant. The groups X and Y complete the structure for cyanines, oxonols or merocyanines in the formula (Scheme 2, at the right side). Therefore, both the addition and removal of two electrons is possible. To test if this general motif is applicable to ring-closed compounds, tetrapyridinium thiophene $\mathbf{4}^{4+}_{OX}$ was prepared, and studied using cyclic voltammetry, spectroelectrochemistry and PM3 calculations covering all five redox states of **4**.

Introduction

In an earlier paper[2] of this series, we proposed a new general structure for electrochromic systems combining the important features of violenes and cyanines according to Scheme 1. While this structure guarantees a stepwise reversible electron transfer typical for violenes,[3] it avoids the problem that the species with the longest wavelength absorption is a radical ion. Instead, as demonstrated by the examples given in parts I,[2] II,[4] and III,[1] the equilibrium concentration of radical ions is minimized, thus leading to an overall transfer of two electrons. Consequently, the colored form is represented by closed shell systems of the cyanine type.

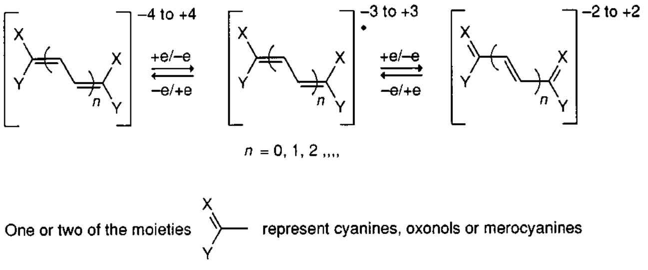

Scheme 1

In Scheme 2 we now present a novel variant of violene/cyanine hybrids as electrochromic systems, which requires a chain of four carbon atoms as the smallest unit since − with regard to the system depicted in Scheme 1 − at both termini, one of the end groups has been moved to the next internal neighbour. In this way, the formula to the far right of Scheme 2 contains two moieties with the structural features of cyanines, oxonols or merocyanines. But now the end groups X and Y are connected by two cross-conjugated trimethine units (or pentamethine units and so on, if vinylogues are employed). These delocalized systems with long-wavelength absorptions may act as either the oxidized or reduced form of a two-step redox system. Therefore, contrasting the basic system of Scheme 1, four electrons may be transferred in total. It is anticipated that the two intermediate radical ions (SEM•) will exhibit a lower thermodynamic stability than in redox systems of the pure violene type.

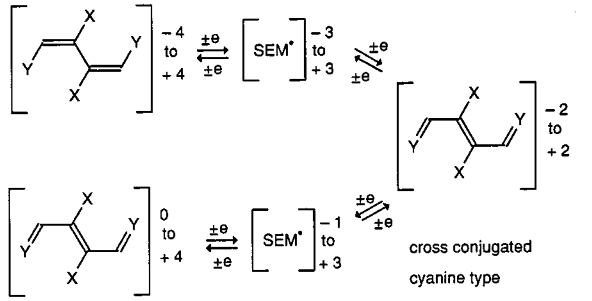

Scheme 2

Before synthesizing and investigating appropriate linear C_4-systems according to Scheme 2, we wanted to check if this general motif can be applied to systems in which the C_4-unit is part of a ring. We therefore decided to prepare and study the tetracation $\mathbf{4}^{+4}_{OX}$.

[‡] Multistep Redox Systems, LXXI. − Part LXX: Ref.[1] − Violene/Cyanine Hybrids as Electrochromic Systems, IV. − Part III: Ref.[1]

[a] Institut für Organische Chemie der Universität Würzburg
Am Hubland, 97074 Würzburg
Fax: (internat.) +49-931/888-4606
E-mail: huenig@chemie.uni-wuerzburg.de

[b] Universität-GH Siegen, Organische Chemie I
Adolf-Reichwein-Strasse, 57068 Siegen
Fax: (internat.) +49-271/740-3270
E-mail: schmittel@chemie.uni-siegen.de

[c] L. M. Litvinenko Institute of Physical Organic & Coal Chemistry, National Academy of Sciences of Ukraine,
R. Luxemburg Street, 70, Donetsk 340 114, Ukraine

[d] MPI für Festkörperforschung
Heisenbergstrasse 1, 70506 Stuttgart

1434−193X/01/0407−1393 $ 17.50+.50/0

Results and Discussion

Tetrakis(1-methyl-4-pyridinio)thiophene (4)

1. Synthesis

The obvious precursor for the quaternary salt $\mathbf{4}_{OX}^{+4}$, i.e. the corresponding tetrapyridinio-thiophene **3**, was already obtained in high yield by varying the conditions of the reaction between 4-methylpyridine and sulfur above 200 °C.[5] The complex events were followed later by analytical methods.[6] Finally, we adopted the synthesis of tetraphenylthiophene from diphenylacetylene and sulfur[7] for the pyridine series. Indeed, 4,4′-dipyridinio-acetylene (**1**), now relatively easily accessible,[8] yielded 28% of **3** in the first run. However, **3** is much more conveniently obtained from the commercially available 4,4′-dipyridinioethene (**2**, starting material for **1**)[8] and sulfur in an unoptimized yield of 48% (after chromatography).

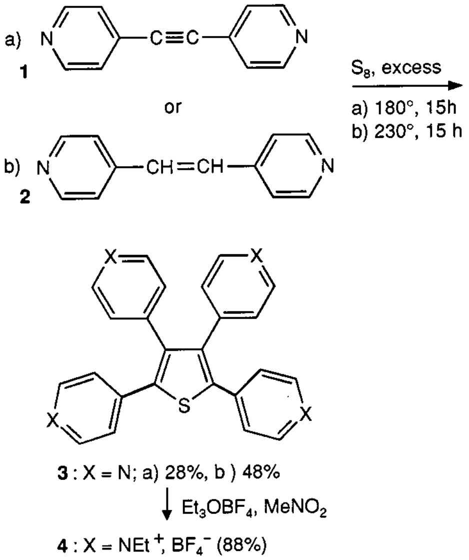

The tetraethylation of **3** to form $\mathbf{4}_{OX}^{+4}$ by triethyloxonium tetrafluoroborate proceeds smoothly (88% yield) if nitromethane is employed as the solvent, since it prevents deposition of the partly quaternized material.

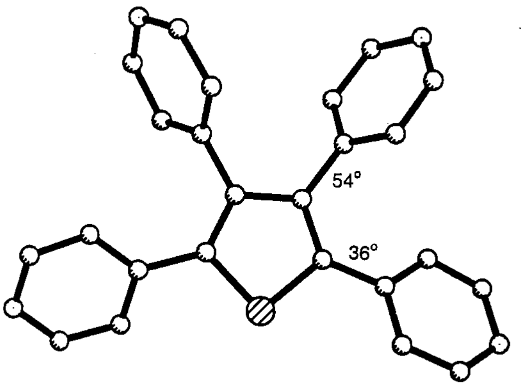

Figure 1. X-ray structure of tetra(4-pyridinoyl)thiophene (**3**)

The structure of **3** was confirmed by X-ray analysis (Figure 1). As expected, the four pyridinyl groups are somewhat twisted out of the plane of the flat thiophene moiety: The two groups close to the sulfur are twisted by 29° ("C2") and 35° ("C5") only, but the other two are twisted by as much as 55° ("C3") and ("C4").

2. Cyclic Voltammogramms (CVs) of System 4

Electroanalytical investigations of $\mathbf{4}_{OX}^{+4}$ tend to provide irreproducible results unless carefully smoothened Pt-electrodes and highly purified solvents are employed. Under these conditions, CVs remain unchanged over several scans indicating two reversible redox processes (Figure 2) with $E_{1/2}$ (1st wave) = −0.54 V (vs. Ag/AgCl) and $E_{1/2}$ (2nd wave) = −0.80 V (vs. Ag/AgCl). With an increased scan rate, the peak separation of the more cathodically shifted wave is increased from ΔE = 65 mV (20 mV s^{-1}) to ΔE = 130 mV (500 mV s^{-1}), while it stays constant at ΔE = 60 mV for the first wave.

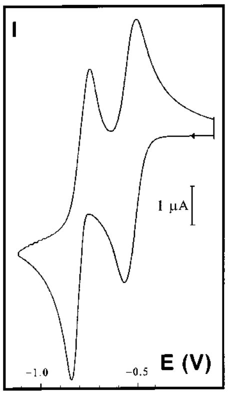

Figure 2. Cyclic voltammogram of the tetracations $\mathbf{4}_{OX}^{+4}$ in MeCN/nBu$_4$NBF$_4$; Pt-working electrode vs. Fe/Fe$^+$

Due to the scan rate dependence, the peak separations cannot be used as unambiguous criteria for the number of electrons transferred in the two redox processes. Hence, we further extended the scan down to −1.7 V and up to +1.2 V, but no other peaks were observed. Using triphenylpyrylium as an internal reference in the cyclic voltammetric investigation, the number of electrons transferred is 1.78 ± 0.07 (1st wave) and 1.98 ± 0.24 (2nd wave). Consequently, the reduction and oxidation peaks in Figure 2 represent the overall transfer of four electrons. As the two 2e$^-$-waves are accompanied by much larger peak separations than expected on theoretical grounds, it is clear that the situation is more complex than Scheme 2 would suggest, most likely because of the spatial changes during the redox process. Therefore the CV of $\mathbf{4}_{OX+}^{4}$ has to be discussed in connection with both the spectroelectrogram (Figure 3) and PM3 calculations (Scheme 3).

3. Spectroelectrogram (SE) of System 4

In Figure 3, the spectral changes are recorded for the stepwise reduction of $\mathbf{4}_{OX+}^{4}$. Two borderline cases can be safely identified: a) $\mathbf{4}_{OX+}^{4}$ before reduction with λ_{max} = 355 nm and no absorption in the visible region (curve 1);

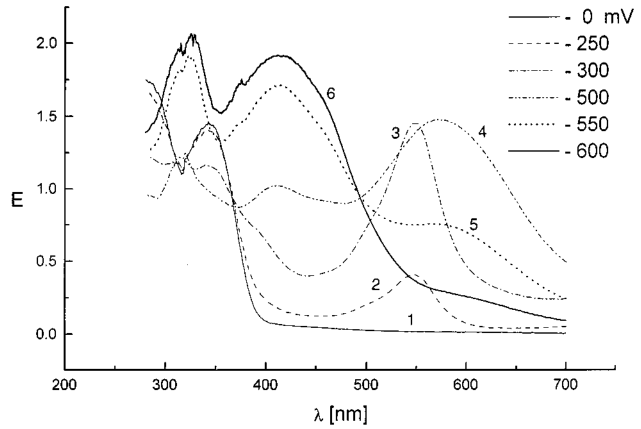

Figure 3. Spectroelectrogram of the tetracation $\mathbf{4}^{+}_{OX}$ in MeCN, *n*Bu4NBF$_4$ Pt. vs. Ag/AgCl (potentials cf. Experimental Section)

and b) the completely reduced form $\mathbf{4}^{0}_{RED}$ since the absorption of curve 6 (340 nm, somewhat structured and 410 nm, broad) retains its pattern even at a more cathodic potential. On reducing $\mathbf{4}^{4}_{OX+}$, an absorption band is first found at approximately 550 nm (curve 2) which on further reduction reaches its highest extinction in curve 3. A different species can be seen in curve 4 which shows a new relatively broad absorption at 570 nm, but already a weak absorption at 410 nm is also observed, indicative of the totally reduced form $\mathbf{4}^{0}_{RED}$. Curve 5 then marks increasing concentrations of $\mathbf{4}^{0}_{RED}$ at the expense of the species ”570 nm”. Curves 1, 2, and 3 on the one hand, and 4, 5, and 6 on the other exhibit rather sharp isosbestic points. In summary, the overall reduction of $\mathbf{4}^{4}_{OX+}$ according to its SE comprises four different species, including the starting material.

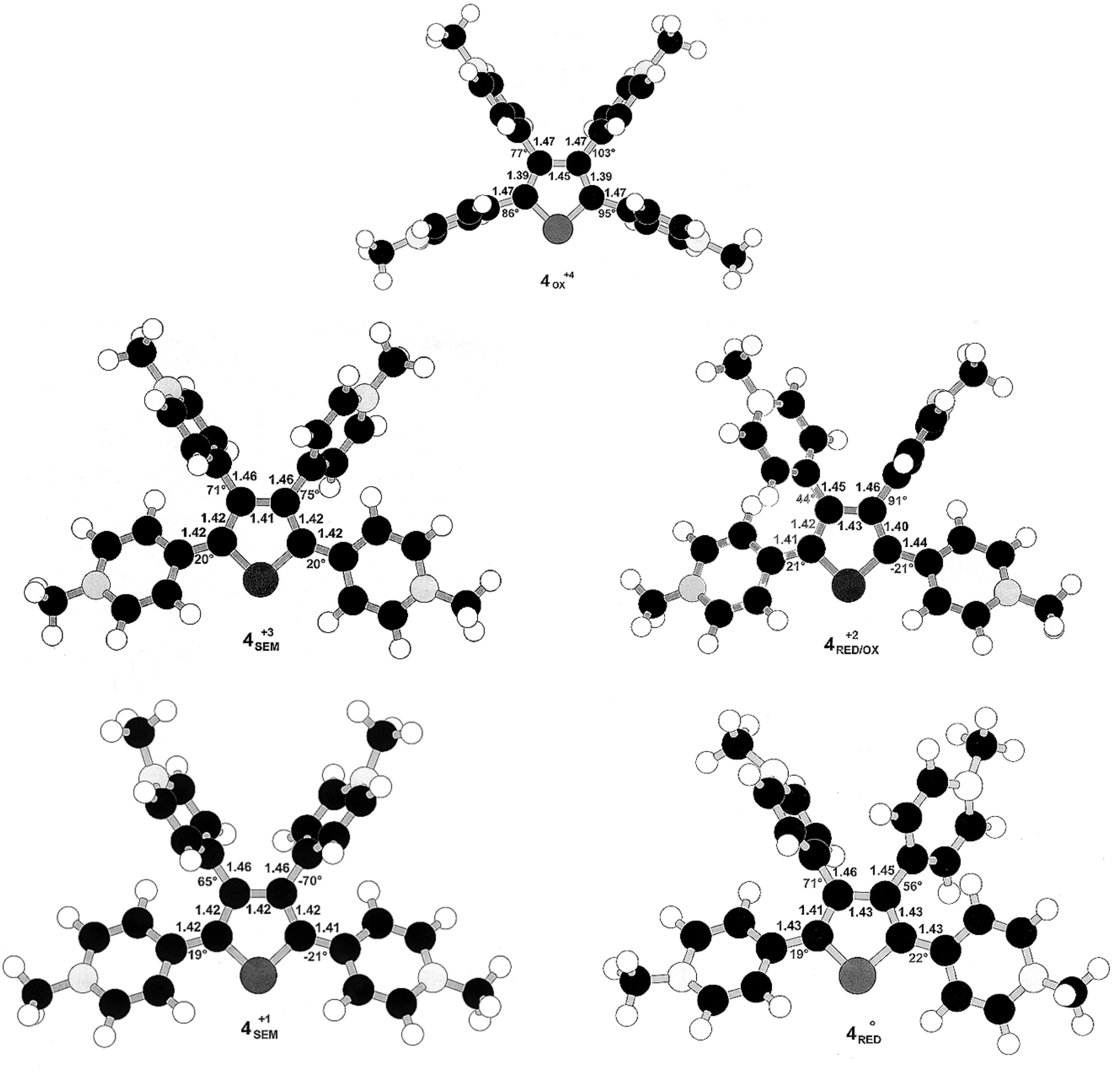

Scheme 3. PM3 calculated geometries of system **4**. *N*-methyl groups with oxidation states +4 to 0

4. PM3 Calculations of System 4

A comparison of the calculated and the experimental ionization energies shows that semiempirical methods[9a,9b] perform better than ab initio (STO-3G, 3-21 G, 6-31G*, 6-31+G**) and DFT (B3PW91, BLYP, B3LYP, B3P86, B3P86)) calculations.[9c] Hence, geometries of all five oxidation states of system **4** were obtained as global energy minima from PM3[9a]/UHF calculations (Scheme 3). The *N*-ethyl groups in **4** were replaced by *N*-methyl groups to simplify the calculation.

In contrast to the X-ray structure of the unquaternized base **3** (Figure 1), all *N*-methyl-pyridinio moieties in $\mathbf{4}^{+4}_{\mathrm{OX}}$ are arranged orthogonally to the thiophene ring. This geometry seems to be favored because it minimizes the repulsion of the partly charged pyridine π-systems. Inspection of the LUMO reveals only significant orbital coefficients at the two central pyridinio groups (at C3 and C4).

Addition of one electron to form $\mathbf{4}^{+3}_{\mathrm{SEM}}$ creates a violene-type radical ion (even number of C atoms between the pyridinio groups) between C2 and C5 of the thiophene ring. Pyridine rings at those positions exhibit only a slight deviation from planarity (20° and 20°, respectively), while the rings at C3 and C4 are tilted by 71° and 75° with respect to the thiophene core. This conformation can be rationalized as the pyridine units close to the sulfur are sterically less hindered to approach co-planarity than those at C3 and C4. Furthermore, the calculations show that another low-energy conformation of $\mathbf{4}^{+3}_{\mathrm{SEM}}$ can be found when the pyridine rings adopt the following dihedral angles (at C2: 38°, at C3: 49°, at C4: −101°, at C5: −72°). In the latter conformation, the violene-type radical cation is found between C2 and C3.

In the dication $\mathbf{4}^{+2}_{\mathrm{RED/OX}}$ the orthogonal pyridinium group at C4 (92°) has no chance to interact. Instead, the HOMO reveals two trimethine cyanine systems, one including atoms C3, C4, and C5, and the other C2, S1, and C5.

Calculations of $\mathbf{4}^{+1}_{\mathrm{SEM}}$ provide a beautifully developed violene-type radical cation from C2 to C5 of the thiophene moiety, with the bond lengths ranging from 1.42−1.41 Å, i.e. between a single (1.47 Å) and a double bond (1.36 Å). However, inspection of the MOs clearly reveals that the molecule has an additional option that is energetically feasible: all spin density could exclusively be located on the pyridine rings at C3 and C4, thus leading to a violene-type radical cation between the central pyridine groups. As these pyridine units are connected by single bonds to the central ring (1.456 Å) and contain bent nitrogen centers, one has to assume that the two 4-positions of the pyridine groups are linked by a long two-center one-electron bond (2.99 Å). Indeed, long bonds in radical cations have been recognized several times.[10]

The last reduction step to $\mathbf{4}^{0}_{\mathrm{RED}}$ causes only a minor change in the structure. As in $\mathbf{4}^{+1}_{\mathrm{SEM}}$, the two pyridine rings at C3 and C4 are more strongly tilted than the thiophene core (71° and 56°, respectively).

To obtain the absolute redox potentials in solution, the solvation energies in acetonitrile were approximated using the Born equation[11] and a mean radius of 6.3 Å. This allows for the calculation of the redox potentials $E°$ [$4^{+n} \rightarrow 4^{+(n-1)}$] from the relative heats of formation in acetonitrile: Reliable data can be expected because only different oxidation states of *one* compound are involved (Table 1). Indeed, the calculations are in good agreement with the experimental cyclic voltammetry data: (1) both the energies of $\mathbf{4}^{+3}_{\mathrm{SEM}}$ and $\mathbf{4}^{+1}_{\mathrm{SEM}}$ are higher than those of $\mathbf{4}^{+4}_{\mathrm{OX}}$ and $\mathbf{4}^{+2}_{\mathrm{RED/OX}}$, respectively, thus suggesting that two $2e^-$-waves should be observed; (2) the two waves should be separated by about 350 mV (experimental value 280 mV); and (3) due to the small difference of 0.04 eV between $\mathbf{4}^{+3}_{\mathrm{SEM}}$ and $\mathbf{4}^{+4}_{\mathrm{OX}}$, some radical ion may be visible in the SE.

Table 1. Absolute redox potentials of $\mathbf{4}^{+n} \rightarrow \mathbf{4}^{+(n-1)}$ obtained from PM3 calculated heats of formation[9a] and solvation energies as derived from the Born[11] equation

	$\Delta H_f°$ (gas phase) [kcal mol^{-1}]	ΔH_{solv} (acetonitrile) [kcal mol^{-1}]	$E°$ [$\mathbf{4}^{+n} \rightarrow \mathbf{4}^{+(n-1)}$] (acetonitrile) [eV]
$\mathbf{4}^{0}_{\mathrm{RED}}$	163.3	= 0	
$\mathbf{4}^{+1}_{\mathrm{SEM}}$	304.0	−25.3	5.00
$\mathbf{4}^{+2}_{\mathrm{RED/OX}}$	492.3	−101.61	4.86
$\mathbf{4}^{+3}_{\mathrm{SEM}}$	741.5	−227.4	5.35
$\mathbf{4}^{+4}_{\mathrm{OX}}$	1040.9	−404.2	5.31

5. Discussion of the Redox Process of System 4

Combining the results from CV, SE, and PM3 calculations, the redox properties of system **4** can be described as shown in Scheme 4. Starting from the tetracation $\mathbf{4}^{+4}_{\mathrm{OX}}$, the first reduction step produces $\mathbf{4}^{+3}_{\mathrm{SEM}}$, a violene radical ranging either from ring A to ring B, or from ring A to ring D. Its absorption maximum at 550 nm may be compared with violene $\mathbf{5}^{+}_{\mathrm{SEM}}$ ($\lambda_{\max}$ = 525 nm[12]). On further reduction, the new species formed can be described as $\mathbf{4}^{+2}_{\mathrm{RED/OX}}$ with a cyanine system ($\lambda_{\max}$ = 570 nm) extending from ring B to ring D, and likewise because of the thiophene ring, from ring A to ring D. The closest analogue could be found for $\mathbf{4}^{+2}_{\mathrm{RED/OX}}$ in the cyclobutane derivative **6** ($\lambda_{\max}$ = 625 nm[13]). Similar to $\mathbf{4}^{+2}_{\mathrm{RED/OX}}$, its absorption maximum is relatively broad, slowly decaying to longer wavelengths. The larger bathochromic absorbance of cyanine **6** than of $\mathbf{4}^{+2}_{\mathrm{RED/OX}}$ may be due to a higher ground-state energy caused by ring strain.

These two first electron transfers are so close together that they are not separated in the CV curve, a well-known feature if less than ca. 50% of SEM are in equilibrium with OX and RED. Accordingly, the observed concentration of $\mathbf{4}^{+3}_{\mathrm{SEM}}$ in the spectroelectrogram is relatively low.

The next redox step in the CV of **4** also represents the transfer of two electrons. Here, a specific absorption of $\mathbf{4}^{+1}_{\mathrm{SEM}}$ is absent in the SE of **4**. Therefore its concentration must be very low, which can be attributed to the large $\Delta\Delta E°$ in the reduction of $\mathbf{4}^{+2}_{\mathrm{RED/OX}}$ and $\mathbf{4}^{+1}_{\mathrm{SEM}}$ (see Table 1). In agreement with this hypothesis, the structural change in the reduction of $\mathbf{4}^{+1}_{\mathrm{SEM}}$ to $\mathbf{4}^{0}_{\mathrm{RED}}$ is relatively small, as indicated by PM3.

The structure of $\mathbf{4}^{0}_{\mathrm{RED}}$ allows for an efficient π-interaction between the four reduced pyridine moieties ($\lambda_{\max}$ ca. 420 nm), since the isolated rings are expected to absorb at

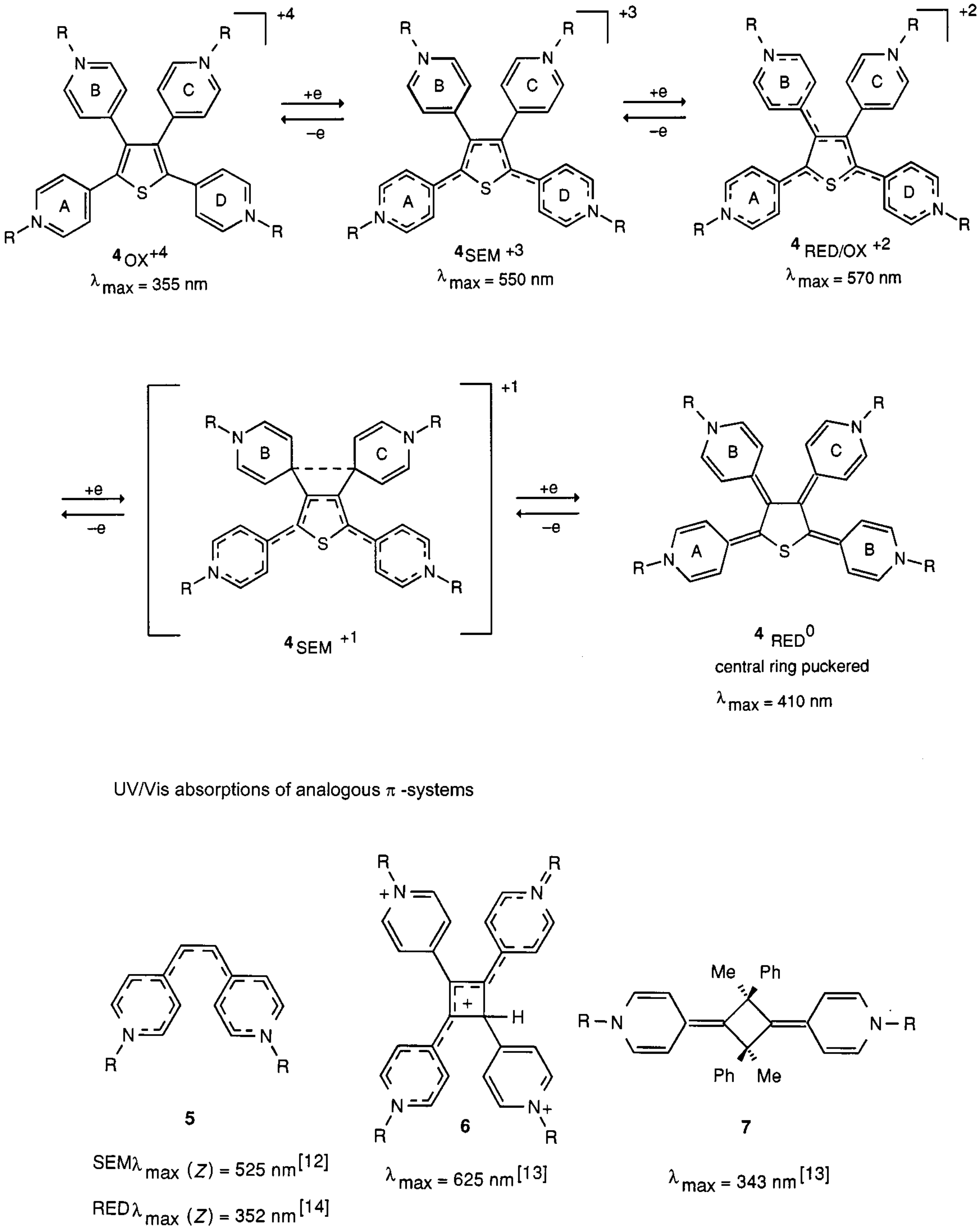

Scheme 4. Redox pattern of system **4** based on its CV (Figure 2) and PM3 calculations (Scheme 3)

approximately 340 nm (cf. model **7**[13]), and coupling between two of them should produce a λ_{max} value of approximately 350 nm (cf. model $\mathbf{5}_{RED}$[12]).

In summary, system **4** can be considered as an example of a violene/cyanine hybrid, according to Scheme 2. However, especially in the case of $\mathbf{4}_{SEM}^{+3}$ and $\mathbf{4}_{SEM}^{+1}$, its behavior is not ideal, probably for steric reasons. In particular, the pyridine units B and C of **4** at C3 and C4 experience unfavorable steric interactions with two equal neighbors. Therefore vinylogues of the general structure as shown in Scheme 2 should not be prone to these drawbacks.

Conclusions

The new variant of violene/cyanine hybrids presented in Scheme 2, in principle allows for the reversible transfer of four electrons, which is observed as a pair of two-electron transfer steps. The differences in absorption are expected to be large enough for electrochromic systems.

With system **4**, all these features could be verified, although not in an ideal way owing to strong steric interactions of the pyridinio groups attached to the rigid thiophene ring.

If the full range of four electron transfers is intended without serious steric effects, systems of the cyanine type on the level RED/OX^{+2} have to be designed according to **8**.

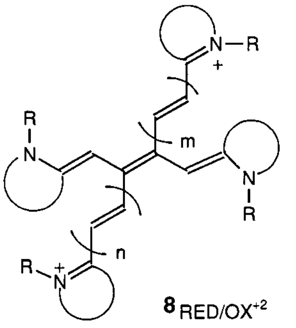

8 RED/OX^{+2}

Systems of that type with two cross-conjugated cyanines have so far not been described, but the general structure of Scheme 2 may inspire a synthesis of these systems, and of similar electrochromics with two interwoven cyanine, oxonol or merocyanine moieties.

Experimental Section

General: Melting points were determined on a heated microscope (Fa. Reichert) and are corrected. – IR: Perkin–Elmer 1420 spectrophotometer. – ^{1}H and ^{13}C NMR: Bruker AC 200 and AC 250 spectrometers; standardized by versus TMS. – MS: Varian MT CH7 and Finnigan MAT 8200 spectrometers. Calculations on Indigo work stations using the force-field program SYBYL[14] and VAMP 5.0.[15]

Electrochemical Measurements

1. Cyclovoltammetry: Electrochemical measurements were performed with an EG&G PAR 273 or a PAR 362 potentiostat. The platinum disk working electrodes had a surface of 0.785 mm^2 (ϕ 1 mm) and were polished down to 0.5 μm (Bühler or Winter polishing paste) prior to use, in order to get a reproducible surface. The counter electrode consisted of a platinum wire, and the reference electrode was a Ag/AgCl wire.[16] For calibration, ferrocene ($E_{1/2}$ = 0.435 V vs. Ag/AgCl) was used. Acetonitrile (LiChrosolv, Merck) and tetrabutylammonium hexafluorophosphate were purified as described earlier.[16]

General Procedure: A solution of $Bu_4N^+PF_6^-$ in MeCN (0.1 M) was deoxygenated with dry argon for 15 min. The corresponding compounds were characterized at a concentration of $1 \cdot 10^{-3}$ M using a scan rate of 100 mV s^{-1}.

Ratios of peak intensities were determined from three experiments using triphenylpyrylium tetrafluoroborate (TTP) as an internal standard (ferrocene and paraquate were not applicable). From a solution of **4** (5.40 μmol) and TTP (10.60 μmol), electron transfer was calculated for the first wave to be 1.78 ± 0.07 e, and for the second wave 1.98 ± 0.24 e.

2. Spectroelectrochemistry (SEs): SEs were recorded on a Perkin–Elmer Spectrophotometer Lambda 19 in conjunction with an EG&G PAR potentiostat, model 363. All optical measurements were carried out at 21 °C in a thin-layer electrochemical cell (distance between working electrode and light conductor: 60 μm) according to Salbeck,[17] incorporating a polished platinum disk electrode (ϕ 6 mm) as the working electrode, an Ag/AgCl wire as the reference electrode, and a platinum sheet as the counter electrode. Spectra were recorded in the reflection mode at the platinum electrode with the aid of a y-type optical fiber bundle.

General Procedure for SE Measurements: To a solution of the substrate (ca. 0.1 mM) in acetonitrile containing Bu_4NBF_4 (0.1 M), the potentials given in the figures were applied and the spectra recorded after equilibration was observed. The potentials do not match those from CV measurements. Differences up to 300 mV occur, owing to the actual geometry of the electrochemical cell used in the specific experiment.

Tetra(4-pyridyl)thiophene (3): In a mortar, 1,2-dipyridylethene (5.00 g, 27.4 mmol) and sulfur (8.78 g, 274 mmol) were carefully mixed. The mixture was heated in a bulb with a bubble counter at 230 °C until the evolution of hydrogen sulfide had ceased (ca. 24 h). The hot dark brown reaction mixture was poured into a mortar, and after solidifying, ground until a fine powder resulted. This product was treated with carbon disulfide (2 × 20 mL) and the remaining brown solid was extracted with dichloromethane (2 × 20 mL). The evaporated solution yielded crude **3** as a brown solid (5.22 g, 97%), m.p. 225–250 °C. This product was again dissolved in dichloromethane. After the addition of basic alox (act. I, 40 g), the solvent was removed. The mixture was loaded on a column filled with dry basic alumina (act. I) and eluted with ethyl acetate/ethanol (95:5). The main fraction was further purified by chromatography in the same way, yielding colorless crystals of **3** (2.60 g, 48%), m.p. 256–258 °C (ref.[5] pale yellow crystals, m.p. 251.8–252.6 °C, no spectral data). – IR (KBr): $\tilde{\nu}$ = 3020 (w), 1584 (s), 1538 (m), 1472 (w), 1408 (s), 1310 (w), 1220 (m), 1090 (w), 1063 (m), 990 (m), 875 (w), 835 (s), 815 (m), 768 (m), 728 (m), 6.65 (w), 613 (m). – ^{1}H NMR (250 MHz, $CDCl_3$, TMS): δ = 6.89 (d, 4 H), 7.08 (d, 4 H), 8.46 (d, 4 H), 8.52 (d, 4 H). ^{13}C NMR (63 MHz, $CDCl_3$, TMS): δ = 123.1 (d, 4 CH), 125.1 (d, 4 CH), 138.1 (s, 2 C), 139.0 (s, 2 C), 140.1 (s, 2 C), 142.6 (s, 2 C), 150.2 (d, 4 CH), 150.4 (d, 4 CH). – MS (70 eV): *m/z* (%) = 392 (100) [M$^+$], 314 (4) [M$^+$ – Py]. – $C_{24}H_{16}N_4S$ (392.5): calcd. C 73.45, H 4.11, N 14.28, S 8.17; found C 72.92, H 4.15, N 13.86, S 7.90.

Tetrakis(1-ethyl-4-pyridinium tetrafluoroborate)thiophene (4): To a solution of triethyloxonium tetrafluoroborate (3.80 g, 20.0 mmol) in dry nitromethane, compound **3** (785 mg, 2.00 mmol) was added. After stirring (2 d) at ambient temperature, excess oxonium salt was destroyed with methanol (1 mL) and the solvent was removed. The residual yellow oil (3.17 g) was solidified on treating with small amounts of methanol, yielding crude **4** (1.51 g, 88%), m.p. 190–195 °C. On cooling a hot solution in ethanol/water (85:15), **4** often deposited as an oil that solidified on grinding. Drying (90–100 °C, 12 h, 0.1 hPa) led to the isolation of **4** (1.16 g, 68%), m.p. 260–270 °C. – ^{1}H NMR (250 MHz, CD_3CN, TMS): δ = 1.59 (t, 12 H), 4.56 (q, 8 H), 7.63 (d, 4 H), 7.81 (d, 4 H), 8.63 (m, 8 H). – $C_{32}H_{36}B_4F_{16}N_4S$ (855.9): calcd. C 44.90, H 4.24, N 6.55, S 3.75; found C 44.69, H 4.27, N 6.49, S 3.83.

Crystal data, data collection, structure solution, and refinement parameters for compound **3** are shown in Table 2.

Table 2. Crystal data, data collection, structure solution, and refinement parameters for compound **3**

Crystallographic Section	
compound	HUE31/We1419
empirical formula	$C_{24}H_{16}N_4S$
molecular mass	392.48
a [Å]	982.8(1)
b [Å]	1903.9(2)
c [Å]	1061.4(1)
β [deg]	104.23(8)
V [pm^3]	$1925.1(4)\cdot 10^6$
Z	4
d(calcr.) [g cm^{-3}]	1.354
crystal system	monoclinic
space group	$P2_1/c$
Data Collection	
diffractometer	Siemens P4
radiation	Mo K_α
monochromator	graphite
crystal size [mm]	0.5 × 0.45 × 0.3
data colledtion mode	ω-scan
theta range [deg]	1.75−27.5
recip. latt. segment	$h = 0 \rightarrow 12$ $k = 0 \rightarrow 24$ $l = -13 \rightarrow 13$
no. refl. measd.	4822
no. unique refl.	4423
no. refl. $F > 3\sigma(F)$	3434
lin. abs. coeff. [mm^{-1}]	0.19
abs. corredtion	ψ-scan
Structural Analysis and Refinement	
solution by	direct phase determination
method of refinement	Full-Matrix LSQ. Hydrogen positions of riding model with fixed isotropic U
data-to-parameter ratio	13.06
R, R_w	0.119, 0.128
weithting scheme	$w = 1/\sigma^2(F)$
largest difference peak	0.28 eÅ^{-3}
largest difference hole	0.31 eÅ^{-3}
program used	Siemens SHELXTL PLUS

Acknowledgments

Financial support by Volkswagen-Stiftung, BASF AG/Ludwigshafen (BMFT project 03 M 4067 6) and Fonds der Chemischen Industrie is highly acknowledged. I.F.P. thanks Alexander von Humboldt-Stiftung for a postdoctoral fellowship (1995−1997) to conduct some of his research work inWürzburg.

---

[1] S. Hünig, I.F. Perepichka, M. Kemmer, H. Wenner, P. Bäuerle, A. Emge, *Tetrahedron* **2000**, *56*, 4203−4211.

[2] Part I: S. Hünig, M. Kemmer, H. Wenner, I. F. Perepichka, P. Bäuerle, A. Emge, G. Gescheid, *Chem. Eur. J.* **1999**, *5*, 1969−1973.

[3] [3a] S. Hünig, *Chimia* **1978**, *32*, 91−93. − [3b] K. Deuchert, S. Hünig, *Angew. Chem.* **1978**, *90*, 927−938; *Angew. Chem. Int. Ed. Engl.* **1978**, *17*, 875−886. − [3c] S. Hünig, H. Berneth, *Top. Curr. Chem.* **1980**, *92*, 1−44. − [3d] For a theoretical comparison of violenes and cyanines, see: St. F. Nelson, H. Q. Tran, M. A. Nagy, *J. Am. Chem. Soc.* **1998**, *120*, 298−304.

[4] Part II: S. Hünig, M. Kemmer, H. Wenner, I. F. Perepichka, P. Bäuerle, A. Emge, K. Peters, *Chem. Eur. J.*, accepted for publication.

[5] H. I. Thayer, B. B. Corson, *J. Am Chem. Soc.* **1948**, *70*, 2330−2333.

[6] E. Gleich, Z. Warnke, J. Szafranek, E. Malinski, *Phosphorus Sulfur* **1986**, *28*, 315−325.

[7] U. Schmidt, K. Kabitzke, K. Markau, A. Müller, *Liebigs Ann. Chem.* **1964**, *673*, 89.

[8] M. Tanner, A. Ludi, *Chimia* **1980**, *34*, 23−24.

[9] [9a] J. J. P. Stewart, *J. Comput. Chem.* **1989**, *10*, 221−264. − [9b] M. J. S. Dewar, E. G. Zoebisch, E. F. Healy, J. J. P. Stewart, *J. Am. Chem. Soc.* **1985**, *107*, 3902−3909. − [9c] P. Politzer, F. Abu-Awwad, *Theor. Chem. Acc.* **1998**, *99*, 83−87.

[10] U. Haberl, E. Steckhan, S. Blechert, O. Wiest, *Chem. Eur. J.* **1999**, *5*, 2859−2865.

[11] P. W. Atkins, *Physikalische Chemie*, VCH Verlagsgesellschaft, Weinheim, **1990**.

[12] A. Slama-Schwok, M. Blanchard-Desce, J.-M. Lehn, *J. Phys. Chem.* **1992**, *96*, 10559−10565.

[13] M. Horner, S. Hünig, *Liebigs Ann. Chem.* **1983**, 642−657.

[14] SYBYL: Tripos Associates, 1699 St. Hanley Road, Suite 303, St. Louis, MO, 63144.

[15] G. Rauhut, J. Chandrasekhar, A. Alex, B. Beck, W. Sauer, T. Clark, *VAMP 5.0* available from Oxford Molecular Limited, The Magdalen Centre, Oxford Science Park, Sandforde on Thames, Oxford 4GA, England.

[16] M. Schmittel, M. Röck, *Chem. Ber.* **1992**, *125*, 1611−1620.

[17] J. Salbeck, *J. Electroanal. Chem.* **1992**, *340*, 169.

Received May 31, 2000
[O00277]